# Supporting Information

## Godec et al. 10.1073/pnas.1413291112

### SI Methods

**In Vitro Knockdown of GFP.** The fraction of protein was calculated as the GFP mean fluorescence intensity (MFI) of the shRNA-transduced relative to the GFP MFI of the untransduced GFP$^+$ Jurkat cells, both normalized to the background fluorescence of the unmanipulated (non-GFP expressing) Jurkat cells.

**Immunoblotting.** CD8$^+$ T cells stimulated in vitro with aCD3/aCD28 were lysed in modified Laemmli buffer [60 mM Tris·HCl (pH 7.2), 10% glycerol, and 2% SDS] containing 1 unit of DNase (benzonase nuclease; Novagen) per microliter and complete protease inhibitor mixture (Roche) for 30 min at 4 °C. Protein concentration in the lysates was estimated with a bicinchoninic acid assay (Thermo Scientific), and 75 μg of each lysate was subjected to SDS-polyacrylamide gel electrophoresis and Western blotting on nitrocellulose membranes as previously described (1). The primary antibodies used were β-actin (1:5,000 dilution; Abcam, ab8227) and BATF (1:500 dilution; Brookwood Biomedical, PAB4003). Densitometry was performed using ImageJ software (National Institutes of Health).

**Flow Cytometry and Cell Sorting.** Single cell suspensions were stained with combinations of anti-CD8α (53-6.7), anti-CD4 (RM4-5), anti-B220 (RA3-6B2), anti-CD11b (M1/70), anti-CD11c (N418), anti-CD44 (IM7), anti-CD62L (MEL-14), anti-CD45.1 (A20), anti-CD45.2 (104), anti-Thy1.1 (OX-7), anti-Thy1.2 (30-H12), anti-CD25 (PC61), anti-CD27 (LG.3A10), anti-CD122 (TM-β1), anti-CD127 (A7R34), anti-CXCR3 (CXCR3-173), anti-TNFα (MP6-XT22), anti-IFNγ (XMG1.2), and anti-Granzyme B (GB11) (all from BioLegend), anti-T-bet (O4-46) and anti-Ki-67 (B56) (from BD Biosciences), anti-Eomes (Dan11mag) (from eBioscience), and anti-KLRG1 (2F1) (from Abcam). Poly-caspase activity was detected using FLICA Vybrant-FAM Assay kit (Life Technologies).

For intracellular cytokine staining, splenocytes were first stimulated with 0.5 μg/mL $GP_{33–41}$ (Genscript) or no peptide for 5 h at 37 °C in the presence of GolgiPlug (BD Biosciences). For intracellular staining of cytokines and Ki-67, the cells were surface stained, fixed/permeabilized, and intracellularly stained using the Foxp3/Transcription Factor Staining Buffer Set (eBioscience) as directed by the manufacturer.

LSK cells were sorted from CD117-enriched bone marrow cells stained with CD117 (ACK2), Sca-1 (D7), and a lineage antibody mixture that included biotin-labeled anti-CD5 (53-7.3), anti-Gr1 (RB6-8C5), anti-B220 (RA3-6B2), anti-CD3e (145-2C11), anti-CD11b (M1/70), anti-Ter-119 (Ter-119), and detected with fluorophore conjugated streptavidin (all from BioLegend). Data were acquired using LSR II or Accuri C6 (BD Biosciences) cytometers and analyzed with FlowJo software (v9.7.2, TreeStar).

**Gene Expression Analysis.** Congenically marked CD8$^+$ T cells were sorted from chimeric mice or following in vitro stimulation. Cells were lysed and RNA was extracted using RNeasy Plus Mini kit (Qiagen). cDNA was generated using High Capacity cDNA Reverse Transcription kit (Applied Biosystems) and analyzed on an ABI 7500 Fast Real-Time Quantitative PCR instrument using gene Taqman probesets from Applied Biosystems.

1. Barnitz RA, Wan F, Tripuraneni V, Bolton DL, Lenardo MJ (2010) Protein kinase A phosphorylation activates Vpr-induced cell cycle arrest during human immunodeficiency virus type 1 infection. *J Virol* 84(13):6410–6424.

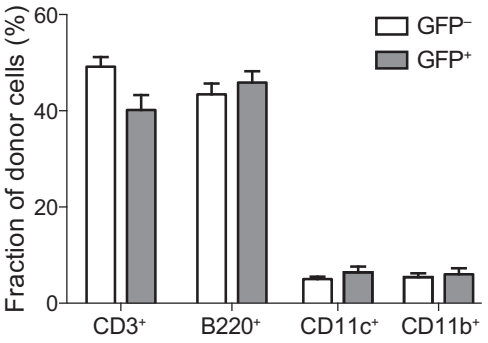


**Fig. S1.** Transduced bone marrow progenitor populations efficiently reconstitute myeloid and lymphoid compartments. [Fraction of indicated donor-derived immune lineages in blood that differentiated from transduced (GFP$^+$) and untransduced (GFP$^-$) congenic WT LSK cells.]

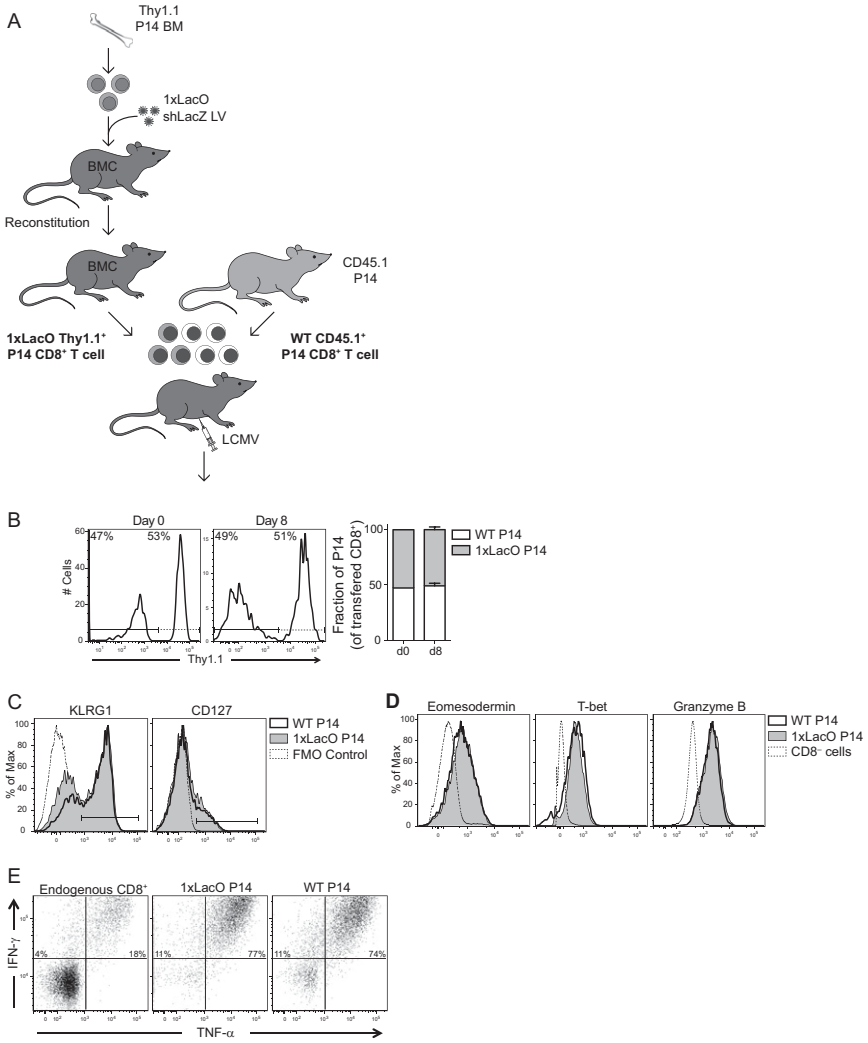


**Fig. S2.** Development from 1xLacO transduced LSK cells does not alter the functional capacity and differentiation of effector CD8$^+$ T cells. (*A*) The experimental schema used to analyze the phenotype of 1xLacO–shRFP-carrying cells relative to unperturbed P14 CD8$^+$ T cells responding early to the LCMV infection. (*B*) The ratio of 1xLacO P14 Thy1.1$^+$ cells and CD8$^+$ T cells directly isolated from the Thy1.1$^-$ CD45.1$^+$ P14 TCR transgenic mouse at the time of injection (d 0) and at d 8 following transfer into mice that were subsequently infected with LCMV Armstrong. Representative plots (*Left*) and summarized data (*Right*). (*C*–*E*) Analysis of effector CD8$^+$ T cells from *B* for their expression of cell surface markers CD127 and KLRG1 (*C*), the transcription factors T-bet and Eomes, and Granzyme B (*D*) as well as their ability to produce cytokines following restimulation with $GP_{33–41}$ peptide (*E*). Data are representative of two independent experiments with 5–10 mice per group.

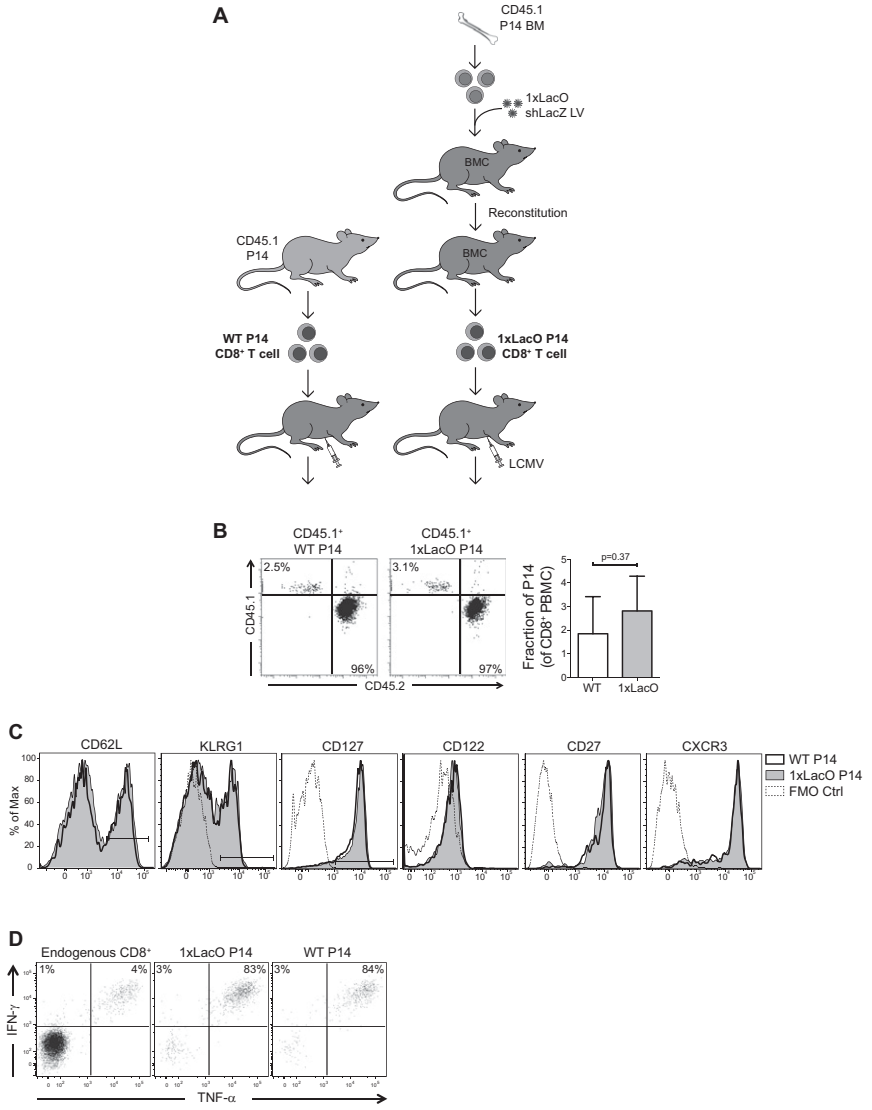


**Fig. S3.** Stable integration of 1xLacO in effector CD8$^+$ T cells does not cause preferential rejection or alter the functional capacity, differentiation, or maintenance of memory CD8$^+$ T cells. (*A*) The experimental schema to assess the memory development of 1xLacO–shRFP-carrying cells and unmodified P14 CD8$^+$ T cells in response to LCMV infection. (*B*) Fraction of transferred 1xLacO P14 cells and unmodified P14 cells at d 28 p.i. Shown are representative plots, gated on total CD8$^+$ T cells (*Left*) and summary data from five mice (*Right*). Statistical significance was assessed using Student's *t* test. (*C* and *D*) Analysis of cells from spleen as in *B* at d 60 p.i. for their expression of cell surface markers (*C*) and ability to produce cytokines upon restimulation with $GP_{33–41}$ peptide (*D*).

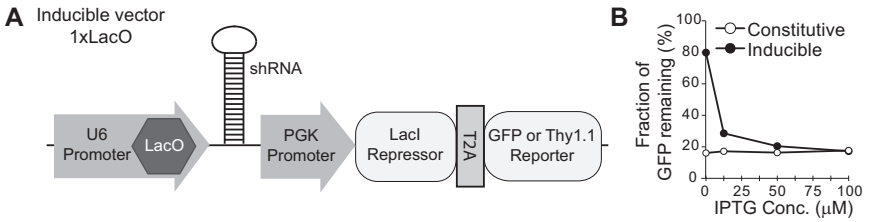


**Fig. S4.** The 1xLacO shRNA vector enables inducible gene knockdown at low IPTG concentrations in vitro. (*A*) Schematic diagram of inducible (1xLacO) vector. (*B*) Fraction of GFP-expressing Jurkat cells transduced with lentivirus expressing an shRNA targeting GFP under constitutive (white symbols) or inducible (black) promoters, cultured with indicated concentrations of IPTG for 7 d.

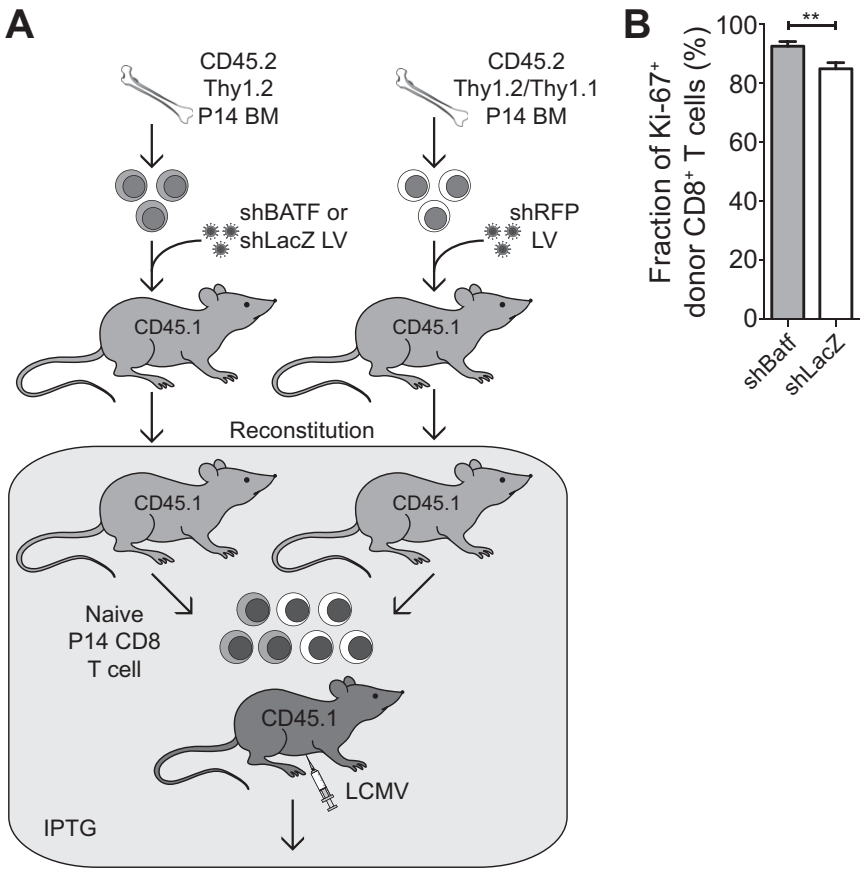


**Fig. S5.** Inducible shRNA-encoding CD8$^+$ T cell transfer enables functional characterization of genes in rigorously naive T cells. (*A*) Schematic diagram of the experiments analyzing competitive advantages of BATF versus control knockdown of CD8$^+$ T cells responding to LCMV infection. (*B*) Ki-67 expression in shBATF and shLacZ effector CD8$^+$ P14 cells on d 5 following cell transfer and LCMV infection. Statistical significance was assessed using Student's *t* test.